



## **Conductive losses in high-frequency strip transmission lines**

Stanley Humphries, Ph.D.

**Field Precision LLC**  
E mail: [techinfo@fieldp.com](mailto:techinfo@fieldp.com)  
Internet: <https://www.fieldp.com>

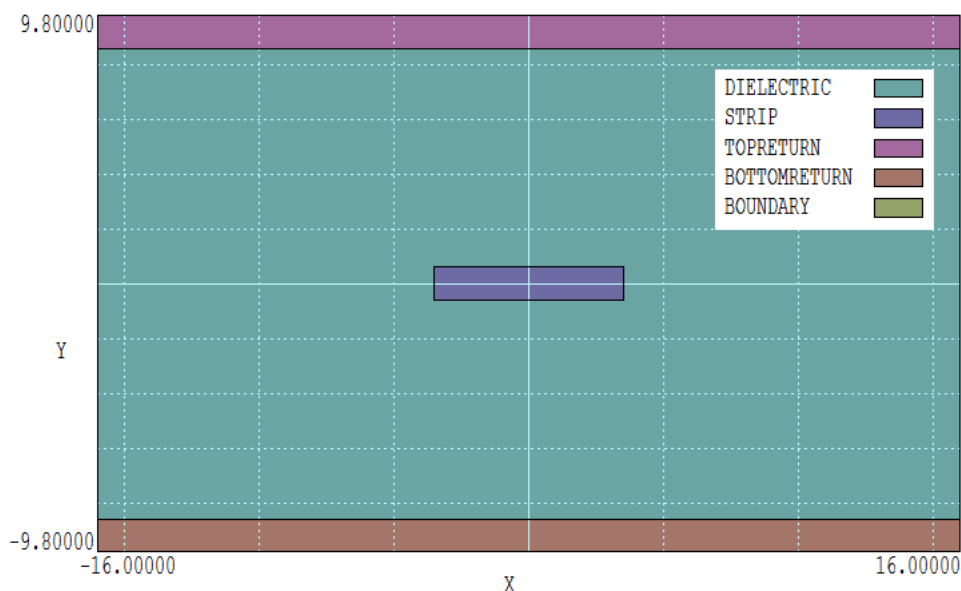


Figure 1: Geometry of the calculation, cross-section of the strip line, dimensions in mil.

A recent LinkedIn post highlighted a report from Simberian Electromagnetic Solutions<sup>1</sup> on conductor losses in strip transmission lines. The process is well described by our **Nelson** code<sup>2</sup> which performs frequency-domain finite-element simulations of magnetic diffusion and eddy current losses. The calculations described in the report provided a good opportunity to make benchmark comparisons and to add a new example to the **Nelson** application library. This report addresses three activities:

- Review the physical formulation and mathematical techniques used in **Nelson**.
- Provide a template for modeling conductive losses in high-frequency transmission lines.
- Illustrate techniques for organizing output data and testing accuracy.

Regarding the Simberian example, power loss and current distribution are probably not concerns in microstrip lines that carry very small currents. On the other hand, the techniques discussed can be applied to transmission lines and bus bars in high-power RF and microwave devices.

<sup>1</sup>Y. Shlepnev, **How Interconnects Work: Modeling Conductor Loss and Dispersion**, 2016, Simberian App. Note 2016\_01.

<sup>2</sup><https://www.fieldp.com/universalbfield.html>

Figure 1 shows a cross-section of the strip line geometry. A rectangular copper strip has dimensions 1.2 mil  $\times$  7.0 mil. The copper return current plates also have thickness 1.2 mil. They are separated from the top and bottom of the strip by an 8.0 mil gap. Before discussing the calculations, it is worthwhile to review some **Nelson** basics.

The governing equation for harmonic variations of magnetic field in the non-radiative limit<sup>3</sup> is

$$\nabla \cdot \left( \frac{1}{\mu} \nabla \mathbf{A} \right) = -\mathbf{J}_0 - \sigma \frac{\partial \mathbf{A}}{\partial t} = -\mathbf{J}_0 - j2\pi\sigma f \mathbf{A}. \quad (1)$$

The validity condition is that real currents are much larger than displacement currents. In the equation,  $\mu$  is the local magnetic permeability,  $\sigma$  is the material conductivity,  $f$  is the excitation frequency and  $\mathbf{J}_0$  is a current density to drive the solution. In the present calculations, all regions have  $\mu = \mu_0$ . For a long transmission line with variations in  $x$  and  $y$  and effectively infinite length in  $z$ , the sole component of the vector potential is  $A_z$ . In this case, the drive current density is in the  $z$  direction ( $J_{0z}$ ) and the electric field and magnetic flux density are given by

$$E_z = -\frac{\partial A_z}{\partial t}, \quad (2)$$

$$B_x = \frac{\partial A_z}{\partial y}, \quad (3)$$

$$B_y = -\frac{\partial A_z}{\partial x}. \quad (4)$$

Equation 2 implies that the final term on the right-hand side of Eq. 1 is  $J_{rz} = \sigma E_z$ , the inductive return current driven by the changing magnetic field.

There is a subtlety in a solution like the present one where a current carrying element with assigned  $J_{0z}$  has non-zero conductivity (and hence non-zero  $J_{rz}$ ). In this case, the total current density is  $J_{tz} = J_{0z} - J_{rz}$ . To initiate a **Nelson** solution, we set the virtual drive current  $J_{0z}$  by specifying the total virtual current of the  $I_{0z}$  conductor. The program divides the value by the cross-section area of the conductor to set the drive current density. The solution gives the actual current carried by the conductor as

$$I_z = \int \int dA (J_{0z} - J_{rz}). \quad (5)$$

Ideally we would like to specify the total current,  $I_z$ , carried by the conductor to initiate the solution, but the magnitude and spatial distribution of the

---

<sup>3</sup>The reference S. Humphries, **Finite-element Methods for Electromagnetics** (<https://www.fieldp.com/femethods.html>) gives a complete derivation.

Table 1: Skin depth as a function of frequency

<b>f (MHz)</b>	<b>Skin depth (mil)</b>
1.0	2.57
10.0	0.812
100.0	0.257
200.0	0.184
1000.0	0.082

return current density is not known in advance. For a calculation with single driven conductor (as the present one), the resolution is simple. We perform a solution with any assigned value of virtual drive current,  $I_{0z}$ , find  $I_z$  from Eq. 5 and then perform a second solution with the drive current adjusted by the normalization factor:

$$I_{0z} \Rightarrow \frac{I_0}{I_z} I_{0z}. \quad (6)$$

Fortunately, the user need not worry about this issue. **Nelson** performs the process automatically when it detects a region with non-zero  $I_{0z}$  and  $\sigma$ . The normalization is more challenging with there are multiple interacting driven conductors that require individual adjustment factors to achieve desired total currents. The theory is described in Section 4.1 of the **Nelson Instruction Manual**<sup>4</sup>. The procedure relies on the linearity of the solutions. If there are  $N$  driven conductors, the code carries out  $N$  initial calculations with normalized drive currents and then performs a matrix inversion to find individual correction factors. Again, the activities in **Nelson** are carried out automatically.

We can now turn to the solutions. The mesh of the initial solutions covers the full region shown in Fig. 1. The element size is 0.1 mil in the strip and nearby return plates with coarser resolution in other regions. The critical parameter in planning runs is the skin depth,

$$\delta = \sqrt{\frac{1}{\pi f \sigma \mu_o}}. \quad (7)$$

Values determined with the **Nelson Skin Depth Calculator** tool are listed in Table 1. Convergence of the finite-element solution requires that skin depth extends over more than two elements. The table indicates that solutions may fail at frequencies above about 50 MHz.

<sup>4</sup><https://www.fieldp.com/manuals/nelson.pdf>

```

1 |* Nelson script (Field Precision)
2 * File: Stripline.NIN
3 * Date: 12/05/2023
4 * Time: 08:07:53
5
6 Mesh = Stripline
7 Geometry = Rect
8 DUnit = 3.9370E+04
9 ResTarget = 5.0000E-08
10 MaxCycle = 5000
11 Freq = 0.2E6
12 * Region 1: DIELECTRIC
13 Material(1) = 1.0000E+00 0.0000E+00
14
15 * Region 2: STRIP
16 Material(2) = 1.0000E+00 5.9600E+07
17 Current(2) = 1.0000E+00 0.0000E+00
18
19 * Region 3: TOPRETURN
20 Material(3) = 1.0000E+00 5.9600E+07
21
22 * Region 4: BOTTOMRETURN
23 Material(4) = 1.0000E+00 5.9600E+07
24
25 * Region 5: BOUNDARY
26 Potential(5) = 0.0000E+00 0.0000E+00
27
28 EndFile

```

Figure 2: **Nelson** input script for a low-frequency solution in the full geometry.

I started at low-frequency to test solution validity and to compare results to theory. The input script created by the **Nelson Solution setup** dialog is shown in Fig. 2. The initial commands specify that the geometry is rectangular, dimensions are interpreted in mils and the frequency is  $f = 0.2$  MHz. All physical regions have  $\mu_r = \mu/\mu_0 = 1.0$ . The dielectric region has zero conductivity and the strip and plates have the conductivity of copper,  $\sigma = 5.96 \times 10^7$  S/m. The solution volume is surrounded by a flux-conserving boundary,  $A_z = 0.0$  (Region 5), where lines of  $\mathbf{B}$  are parallel at the periphery. This choice is not ideal if the goal is a solution in infinite space, but the alternative Neumann condition (lines of  $\mathbf{B}$  normal to the periphery) is non-physical. I shall discuss boundary effects in more detail later.

With a normalized drive current amplitude of 1.0 A, the total current density has an average value of  $1.845 \times 10^8$  A/m<sup>2</sup>, uniform to within 0.13% over the width. In the standard analysis configuration, **Nelson** can calculate and record integrals of several quantities over the cross-section. The code finds an integrated power loss in the strip per length in  $z$  of 1.5483 W/m. We can compare this to the analytic prediction. The cross-section area of the 1.2 mil by 7.0 mil bar of  $5.4193 \times 10^{-9}$  m<sup>2</sup>. Dividing the conductivity of copper by this value gives a resistance per length of  $r = 3.0961$   $\Omega$ /m. The predicted power loss per length is

$$p = \frac{I^2 r}{2} = 1.5480 \quad (\text{W/m}). \quad (8)$$

Another quantity of interest is the total current in conductive regions,

$$I_z = \int \int dA \sqrt{2\sigma p}. \quad (9)$$

**Nelson** determines the amplitude of current in the strip as 1.000094 A, but the amplitude of return current in the upper and lower plates is only 0.0348 A. This appears a bit mysterious until we consider the effect of the boundaries. A flux conserving boundary acts as though the solution volume were surrounded by a superconductor. The boundary carries an effective surface current density that causes the magnetic flux density outside to drop to zero. At frequencies where the skin depth is large compared to the plate thickness, almost the full intensity of  $\mathbf{B}$  reaches the boundary. In this case, the boundary carries most of the return current. On the other hand, at high frequency where the skin depth is small compared to the plate thickness, the full drop of magnetic flux density occurs across the plate. Here, we expect to find that the integral of return current in both plates approaches an amplitude close to 1.0 A. For example, at 50 MHz with a drive current amplitude of 1.0 A and phase  $0.0^\circ$ , the plates carry a return current of 0.90 A with phase  $179.97^\circ$ . Figure 3 shows the corresponding current density distribution. Note that values in the plate have been multiplied by a factor of 6 for visibility. The current in the strip has been forced to the ends. The current in the plate extends over a length a few times the strip width and is confined to a skin depth. Figure 4 shows a plot of conductive power loss per length in the strip and return plates. The dashed line is the theoretical zero-frequency value. Losses increase with frequency because the current is confined over a smaller area. Power loss in the plates is negligible at low frequency but approaches a value of about 18% of the strip loss when the skin depth is smaller than the plate thickness.

Smaller elements are required to investigate a broader range of frequency. We can modify the setup in two ways to reduce the run time.

- The main interest is in the current distribution and power loss in the center strip, so we will eliminate the plates, replacing them with a flux-conserving boundary.
- The geometry of Fig. 1 is redundant. By symmetry, we need model only one quadrant.

We will represent the first quadrant with the natural Neumann condition (lines of  $\mathbf{B}$  normal to the surface) on the left and bottom boundaries. The

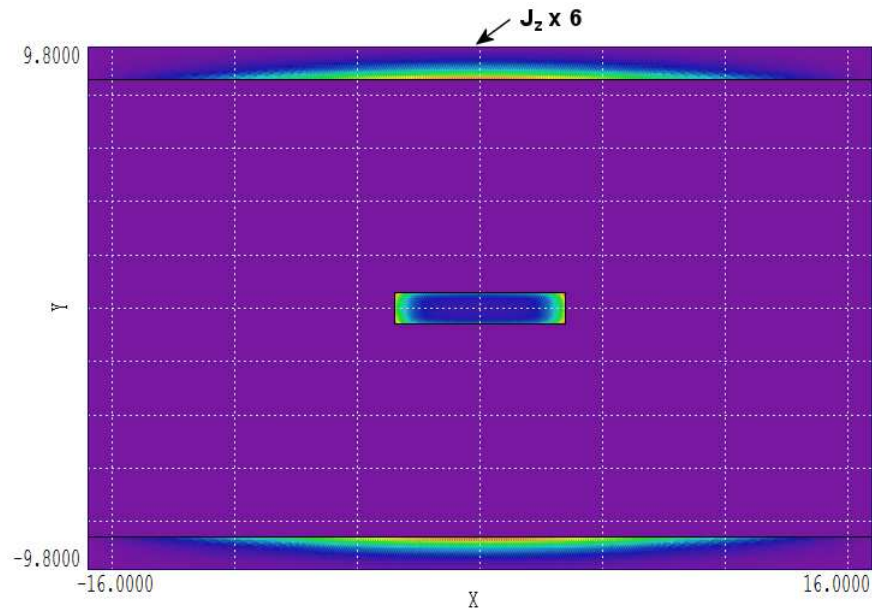


Figure 3: Current density distribution in the strip line at  $f = 50$  MHz. Values in the return plates have been multiplied by a factor of 6 for visibility. Nelson input script for a low-frequency solution in the full geometry.

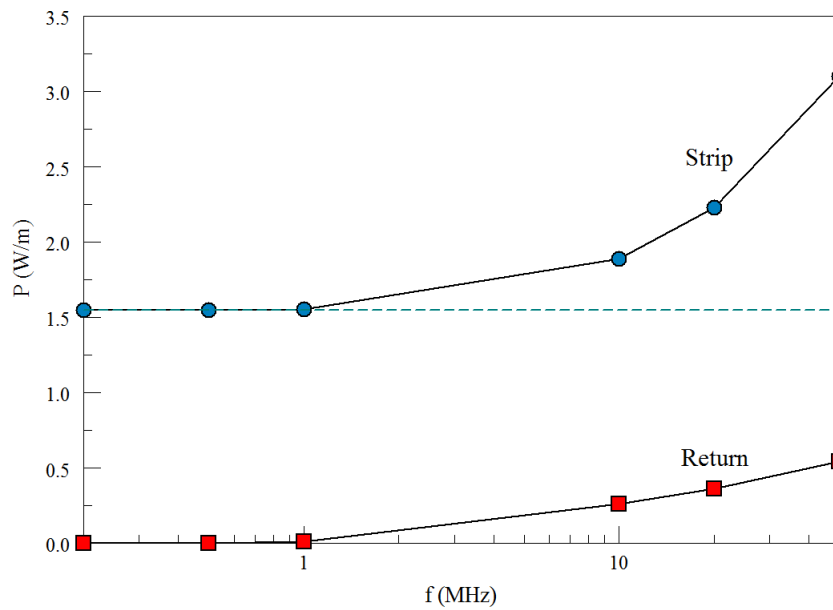


Figure 4: Conductive power loss per length as a function of frequency in the strip and return plates. The dashed line is the theoretical DC value.

Dirichlet condition  $A_z = 0.0$  (where lines of  $\mathbf{B}$  are parallel to the surface) applies on the upper and right boundaries. Second, we reduce the element size in the strip to 0.025 mil, allowing good representation of narrow skin depths. With this choice, the calculation is stable to 500 MHz. Figure 3 shows how the distribution of current density in the strip varies with frequency. The flow is uniform at low frequency but the current density is pushed to the outer edges of the strip as frequency increases, consistent with the Simberian results. At 500 Mhz, the current density on the top is confined to a uniform layer of thickness  $\delta$ , but with significant enhancement on the end. Figure 6 shows the effect of eddy currents on the magnetic flux density  $\mathbf{B}$  at low and high frequency. Finally, Figure 7 shows the enhancement of power loss over a broad frequency range. Here, the code results are multiplied by 4.0 to account for the other quadrants. The values below 100 MHz are in good agreement with those of Figure 4. The integral of the time-averaged magnetic field energy  $U$  can be used to infer the inductance per unit length,  $L$ . The energy integral at 500 Mhz is about 85% of the low-frequency value because of field exclusion from the strip. The prediction is that the characteristic impedance of the line is about 8% higher at low frequency. In the calculations of this report, the dielectric between electrodes was taken as ideal. The **RFE2** code<sup>5</sup> can be employed to find stripline power losses with imperfect dielectrics.

---

<sup>5</sup><https://www.fieldp.com/rfe2.html>



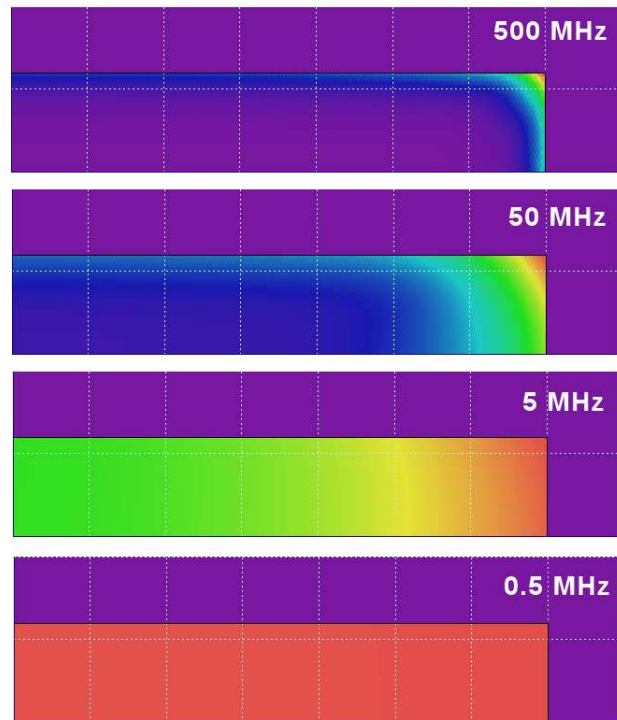


Figure 5: Relative current density distribution in one quadrant of the strip as a function of frequency.

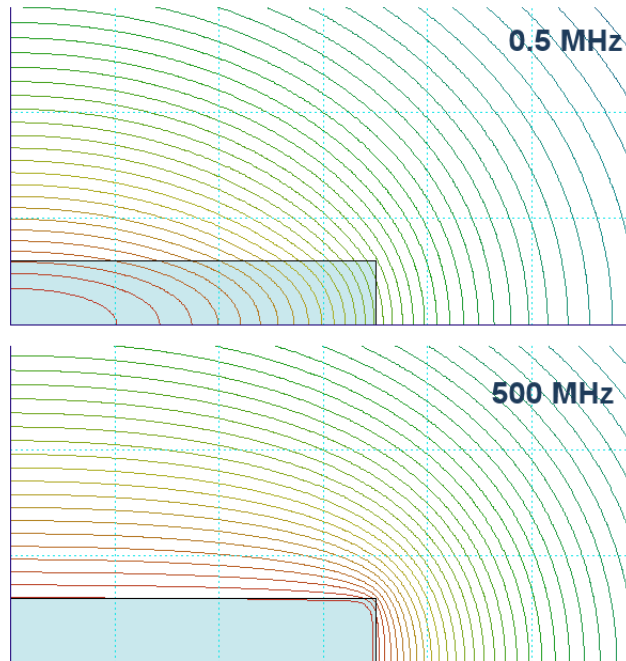


Figure 6: Lines of magnetic flux density  $\mathbf{B}$  at low and high frequency. The Neumann condition applies on the left and bottom edges.

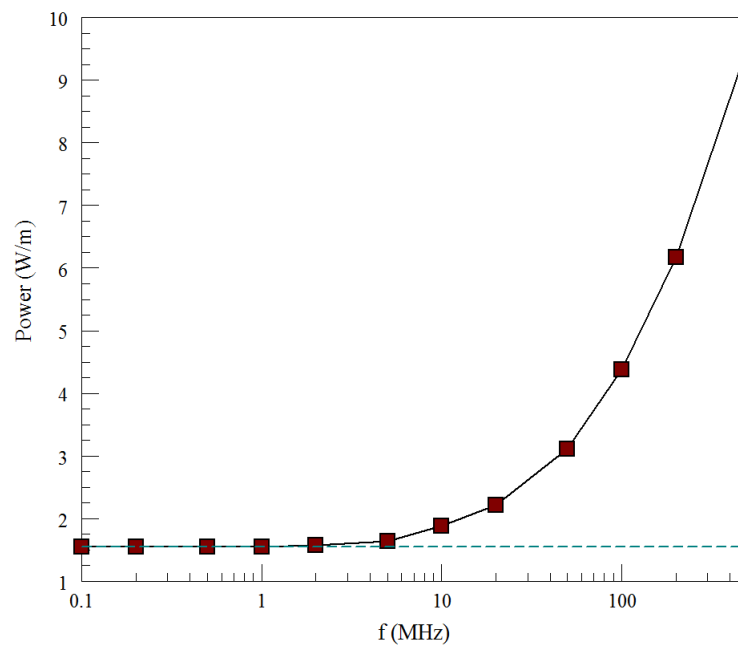


Figure 7: Power loss per length in the strip as a function of frequency. The dashed line is the theoretical DC value.